DFT Study of Ethylene and Propylene Copolymerization over a Heterogeneous Catalyst with a Coordinating Lewis Base

Zygmunt Flisak[†,‡] and Tom Ziegler*[,†]

Department of Chemistry, University of Calgary, 2500 University Drive, Calgary, AB T2N-1N4, Canada, and Institute of Chemistry, University of Opole, Oleska 48, 45-052 Opole, Poland

Received July 29, 2005; Revised Manuscript Received August 31, 2005

ABSTRACT: The copolymerization of ethylene and propylene over a heterogeneous Ti(III) catalyst containing tetrahydrofuran (THF) as a Lewis base and $MgCl_2$ as a support has been studied by means of DFT. Two feasible models of active sites have been examined thoroughly, and one of them turned out to be favorable in terms of both catalytic activity and the microstructure of the resulting polymer. The external barriers of olefin insertion for this model range from 3.1 to 16.0 kcal/mol and are influenced by a variety of factors, such as the structure of the growing polymer chain and the nature of the incoming olefin as well as the orientation of the ligands around the titanium atom. Stochastic simulations performed on the basis of insertion and termination barriers provided us with the insight into the composition and microstructure of the copolymer as well as its molecular weight as a function of comonomer partial pressures. It is demonstrated that the reactivity of ethylene in the copolymerization process is significantly higher than that of propylene, which is consistent with known experimental data. Our results also indicate moderate regiospecificity and stereoselectivity toward propylene, depending on the partial pressures of the comonomers.

Introduction

Polymerization of α-olefins by heterogeneous Ziegler−Natta (ZN) catalysts still counts for most of the polyethylene and polypropylene produced industrially. Despite the spectacular discoveries in the field of metallocene and postmetallocene systems, there are technological obstacles that prevent their widespread commercial application.

The number of recent theoretical papers dealing with the classical Ziegler−Natta systems[1−11] is relatively small in comparison to the number of studies devoted to homogeneous systems. Copolymerization of ethylene and propylene by a second-generation ZN catalyst based on $TiCl_3/MgCl_2$ has been studied recently by theoretical methods.[1] A number of plausible active sites were chosen, and the growing polymer chain was modeled by methyl, propyl, 2-butyl, and isobutyl groups to simulate the different polymer segments that might occur near the metal center during copolymerization. This model had only academic interest since it by design omitted any use of bases. Such bases are in industrial processes coordinated directly to the metal center or situated in its vicinity. The results indicated that, in contrast to industrial processes where bases are used,[12] propylene was more readily inserted into the Ti−C bond than ethylene. It is thus clear that the use of a base has a significant influence on the copolymerization. This will be the subject of the current investigation.

We decided to deal with two models of the catalyst in which a titanium(III) species is deposited on the relaxed (100) and nonmodified (110) surfaces of a $MgCl_2$ crystal, referred to as the "slope" and "edge" models in refs 1−3 (see Figure 1). These models of active sites were obtained from an extensive series of systematic studies. First, it was found that all potential Ti(IV) sites were prone to poisoning by THF. In the next step, three models (namely "slope" , "edge", and "Corradini") were created by adding $TiCl_3$ to a $MgCl_2$ surface.[3] Then, THF was added to all the models,[2] resulting in—according to the calculations—poisoning of the "Corradini" model,[2] which excludes it from further consideration within this work. It is worth noting that poisoning of this model by other Lewis base, di-*n*-butyl phthalate, was also reported earlier.[6]

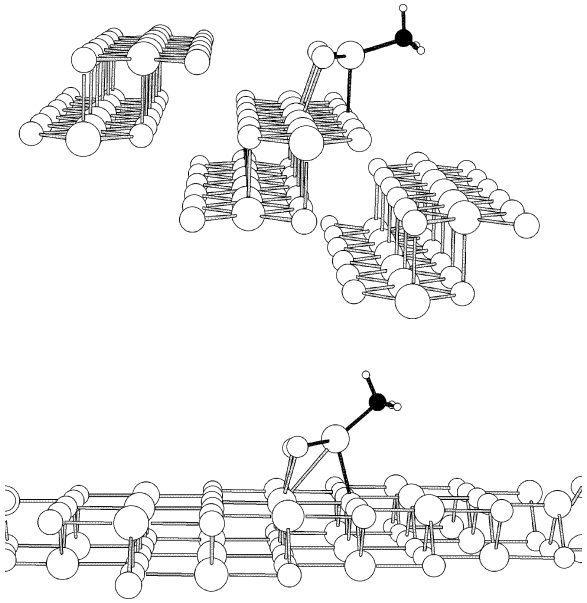

Figure 1. Ti(III) sites within the "slope" and "edge" models.

The remaining models discussed within this paper contain the molecule of THF coordinatively bound to the transition metal atom, since there is certain experimental evidence[13] that a molecule of Lewis base is attached to the active site. In our case, two possible orientations of THF, referred to as front and back, give rise to different starting frameworks for the active sites and

† University of Calgary.
‡ University of Opole.
* Corresponding author. E-mail: ziegler@ucalgary.ca.

10.1021/ma0516844 CCC: $30.25
Published on Web 10/05/2005

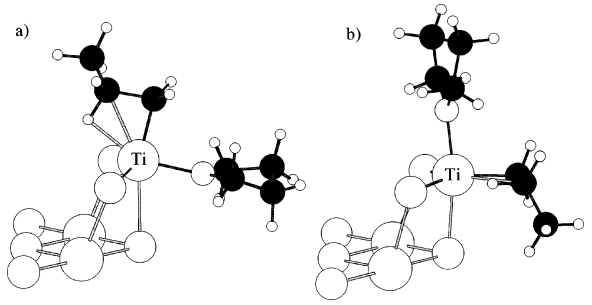

Figure 2. Bare catalytic sites within the "slope" model: (a) THF-back and (b) THF-front. For the sake of clarity, most of the support atoms have been omitted.

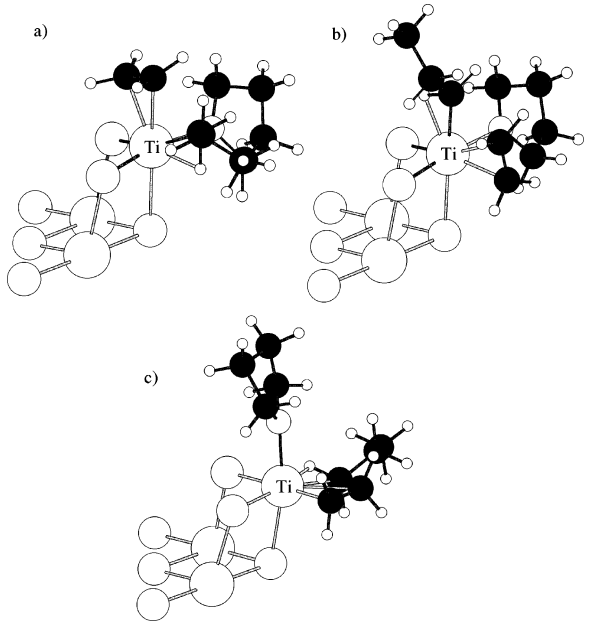

Figure 3. Insertion transition states for the "slope" model: (a) THF-back-ethylene-front; (b) THF-back-ethylene-back; and (c) THF-front-ethylene-back.

transition states, which are shown in Figure 2. Furthermore, one possible mode of olefin coordination for the former and two for the latter result in three separate combinations: THF-back-olefin-front, THF-back-olefin-back, and THF-front-olefin-back (see Figure 3). Since propylene is a prochiral monomer, four distinct orientations corresponding to 1,2-insertion and 2,1-insertion as well as *re*- and *si*-enantiofaces should also be considered (see Figure 4). Such a treatment leads to 90 insertion and 90 termination barriers to be calculated, since there are—as mentioned—two different models, three sites with three different alkyl groups attached to the titanium atom for each model and five possible monomer orientations (including ethylene). The three alkyl groups (*n*-propyl, 2-butyl, and isobutyl) simulate the different possible end groups during the copolymerization.

The values of the insertion and termination barriers obtained from DFT calculations are applied in a stochastic simulation of the polymerization process. In the first step of this procedure, productivity is calculated, which makes it possible to exclude the "slope" model from further consideration due to its low activity. The next stage of the stochastic approach affords the information related to stereospecificity and stereoregularity of the "edge" model, which has remarkable contribution to the polymerization process. Finally, the microstructure of the resulting polymer as well as molecular

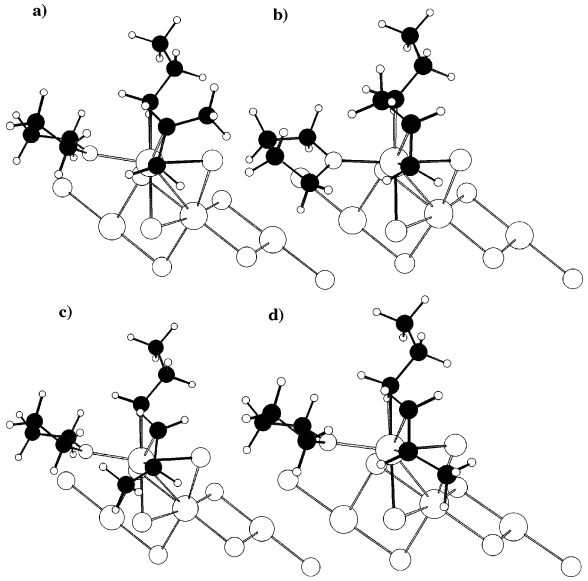

Figure 4. Insertion transition states for the "edge" model (THF-back-olefin-front site) showing four possible orientations of propylene: (a) 1,2-insertion, *re*; (b) 1,2-insertion, *si*; (c) 2,1-insertion, *re*; (d) 2,1-insertion, *si*.

weight and its distribution predicted by the stochastic simulations is analyzed and discussed.

Computational Details

The procedures of quantum-mechanical calculations are similar to those described in refs 1−3; therefore, only a brief outline will be given in this paper. The active sites, the polymer, monomers, and THF were described using DFT. A combined quantum mechanical/molecular mechanical (QM/MM) approach was used to describe the surface of the support. The functional used in all DFT calculations was made up of the exchange correction by Becke[14] and the correlation correction by Perdew[15] with the Vosko, Wilk, and Nusair parametrization of the electron gas.[16] A valence triple-ζ Slater-type orbital (STO) basis set was applied to the Ti atom, while for the Mg, Cl, C, O, and H atoms a double-ζ basis sets were used. In addition, the Mg, Cl, O, and C basis sets are supplemented by one 3d polarization function and the H basis set includes a 2p polarization function. The molecular density and the Coulomb and exchange potentials were fitted using an auxiliary s, p, d, f, and g set of STO functions[17] centered on each nucleus. The core definitions used to decide which orbitals to keep frozen were [Ne] for Ti, Cl, Al, and Mg and [He] for C and O. The convergence criteria for geometry optimizations were 0.0001 au in the energy and 0.001 au $Å^{-1}$ or au rad^{-1} in the gradient. The integration parameter used was 5.0. Transition states were located by varying the C_1 to C_α bond distance as reaction coordinate (RC). The transition state was taken to be at the geometry where the energy was a maximum with respect to variations of RC, and all forces were less than the quoted tolerances. The MM part of the QM/MM calculations is identical to that utilized in the previous work.[2] Geometry optimization and vibrational analysis were performed using the ADF 2002 program.[18−22]

The source code of the generator of uniform deviates applied in the stochastic simulation was based on the example *ran2* given in ref 23. Simulations were performed for the temperature of 323.15 K. The maximum degree of polymerization was set to 1.0×10^6, but it

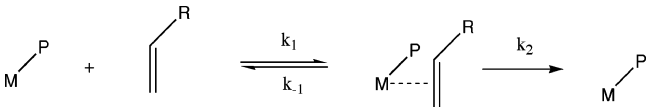

Figure 5. Polymerization reaction.

usually reached lower values due to the termination reaction. For the sake of statistical confidence, the simulation was repeated 1000 times for each site, and the average numbers were taken into account.

Energetic Profiles of Insertion and Termination

The geometries of the transition states of ethylene and propylene insertion for the "slope" and "edge" models with three different alkyl chains (*n*-propyl, 2-butyl, and isobutyl) that simulate the growing polymer chain as well as three different relative orientations of THF (THF-back-olefin-front, THF-back-olefin-back, and THF-front-olefin-back) were all optimized. Selected structures are given in the Supporting Information. Additionally, the geometries of the respective π-complexes were also optimized.

The rate r of olefin polymerization corresponding to the process shown in Figure 5 is given by

$$r = \frac{k_1 k_2 [\mathrm{C}_n\mathrm{H}_{2n}][\mathrm{M}]}{k_1[\mathrm{C}_n\mathrm{H}_{2n}] + k_{-1} + k_2} \quad (1)$$

where k_1 is the rate constant of π-complex formation, k_2 is the rate constant of insertion, and k_{-1} is the rate constant of olefin dissociation from the π-complex. Finally, $[\mathrm{C}_n\mathrm{H}_{2n}]$ and [M] are the concentrations of the olefin and the catalyst, respectively. For the systems considered here, the π-complex formation is endoenergetic. Thus, $k_{-1} \gg k_2$ and also $k_{-1} \gg k_1[\mathrm{C}_n\mathrm{H}_{2n}]$, which makes it it possible to approximate r as

$$r = \left(\frac{k_1}{k_{-1}}\right) k_2 [\mathrm{C}_n\mathrm{H}_{2n}][\mathrm{M}] \quad (2)$$

where the factor k_1/k_{-1} is the equilibrium constant between the olefin π-complex and the reactants from which it is formed: free olefin and the catalyst with the alkyl chain attached.

Making use of the Eyring equation for the rates k_1, k_{-1}, and k_2, we obtain the rate of polymerization for a certain system:

$$r_{a,b} = \frac{kT}{h} \exp\left(\frac{-\Delta G^{\#}_{a,b}}{RT}\right) [\mathrm{C}_n\mathrm{H}_{2n}][\mathrm{M}] \quad (3)$$

Here $\Delta G^{\#}_{a,b}$ is the free energy of activation relative to the alkyl complex and free olefin. For a given alkyl chain ($a = 1$: *n*-propyl; $a = 2$: 2-butyl; $a = 3$: isobutyl) the free energy of activation is calculated with respect to the most stable conformation of the olefin-free alkyl complex, which has THF in the front position. The index b runs over different insertion transition states ($1 \le b \le 15$), depending on the monomer (ethylene or propylene), orientation of the olefin relative to THF (THF back, olefin front; THF back, olefin back; THF front, olefin back), orientation of propylene (*re* vs *si*), and insertion mode of propylene (1,2- vs 2,1-).

In the following stochastic treatment we shall only need relative rates $r_{a,b}/r_{a,b'}$ for the same chain a with different transition states b and b'. Assuming that the entropy contribution $\Delta S^{\#}_{a,b}$ to $\Delta G^{\#}_{a,b} = \Delta E^{\#}_{a,b} - T\Delta S^{\#}_{a,b}$ is nearly the same for b and b', we only need to calculate $\Delta E^{\#}_{a,b}$. The calculated activation energies $\Delta E^{\#}_{a,b}$ for $1 \le a \le 3$ and $1 \le b \le 15$ are given in Table 1. We shall in the following refer to $\Delta E^{\#}_{a,b}$ as the external barrier since it is calculated with respect to free ethylene and the alkyl complex in its most stable conformation (THF in the front position), rather than the internal barrier relative to the olefin π-complex.

From the values of the external insertion and termination barriers, for all models and sites investigated, it is obvious that different productivity, regioselectivity,

Table 1. External Barriers of Insertion and Termination for the "Edge" Model

olefin and THF coordination	olefin	orientation	insertion mode	$\Delta E^{\#}_{a,b}$,[a] kcal/mol	$\Delta E^{\#}_{T}$, kcal/mol
		n-Propyl Chain			
THF-back-olefin-front	ethylene			3.1	9.5
	propylene	*si*	1,2	6.1	11.0
	propylene	*si*	2,1	7.0	11.5
	propylene	*re*	2,1	7.1	12.6
	propylene	*re*	1,2	7.6	12.4
THF-back-olefin-back	ethylene			3.3	11.2
	propylene	*si*	1,2	4.7	12.1
	propylene	*re*	1,2	6.8	13.5
	propylene	*re*	2,1	8.0	12.0
	propylene	*si*	2,1	12.9	12.5
THF-front-olefin-back	ethylene			4.5	17.4
	propylene	*re*	1,2	5.5	22.7
	propylene	*re*	2,1	7.7	23.8
	propylene	*si*	1,2	9.1	23.5
	propylene	*si*	2,1	10.4	20.0
		2-Butyl Chain			
THF-back-olefin-front	ethylene			7.2	10.6
	propylene	*si*	2,1	11.0	12.6
	propylene	*re*	2,1	12.1	12.1
	propylene	*si*	1,2	12.6	12.1
	propylene	*re*	1,2	12.9	13.4
THF-back-olefin-back	ethylene			6.7	10.4
	propylene	*re*	1,2	9.9	13.3
	propylene	*re*	2,1	11.4	12.3
	propylene	*si*	1,2	11.8	12.5
	propylene	*si*	2,1	16.0	13.5
THF-front-olefin-back	ethylene			8.4	17.7
	propylene	*re*	2,1	12.1	22.3
	propylene	*si*	1,2	12.8	24.3
	propylene	*re*	1,2	13.6	22.9
	propylene	*si*	2,1	15.3	24.1
		Isobutyl Chain			
THF-back-olefin-front	ethylene			6.1	8.5
	propylene	*re*	2,1	9.6	11.7
	propylene	*si*	2,1	10.0	10.6
	propylene	*re*	1,2	10.8	11.3
	propylene	*si*	1,2	11.0	11.8
THF-back-olefin-back	ethylene			5.2	11.0
	propylene	*si*	1,2	6.9	13.9
	propylene	*re*	1,2	9.1	13.6
	propylene	*re*	2,1	9.6	14.5
	propylene	*si*	2,1	15.0	13.8
THF-front-olefin-back	ethylene			5.1	22.2
	propylene	*re*	2,1	8.3	28.2
	propylene	*re*	1,2	8.4	29.3
	propylene	*si*	1,2	10.1	25.7
	propylene	*si*	2,1	11.2	22.5

[a] The energies of the barriers were all relative to the bare site (without olefin) of the lowest energy, i.e., the one with THF in the front position.

and stereospecificity can be expected for individual active sites, even within the same model. However, some common trends are conspicuous.

In particular, the active sites built using the "edge" model show significantly lower insertion barriers than the ones within the "slope" model, which implies their higher activity. This is caused by the extent of steric hindrance exerted by the support on the ligands, especially the molecule of olefin. In the "slope" model, the ligands interact with two (or even three) layers of $MgCl_2$ crystal, arranged below and above the titanium atom, whereas only one flat layer of the support is exposed in the "edge" model. The other factor which brings about the differences in activity is the interaction of the incoming olefin molecule and the growing polymer chain with two chlorine atoms attached to the titanium atom. The Cl−Ti−Cl angle equals only 93° in the "edge" bare site with THF in the front position and 123° in the analogous "slope" site, which makes the latter significantly more crowded and less active toward the insertion. For this reason, we have selected only the "edge" model as a subject to the stochastic approach. The decision to drop the "slope" model from the discussion is based on a full stochastic treatment with both the "slope" and "edge" models included. It was shown from this treatment that the "slope" contributes little to the polymer production.

Furthermore, in every case, ethylene tends to be more reactive than propylene, which is consistent with experimental results for base-added catalysts.[12] Certain sites, such as THF-back-olefin-back, clearly favor 1,2-insertion, whereas 2,1-insertion is preferred in the case of the THF-back-olefin-front, independently of the model of the active site and the growing polymer chain attached to it. This is the result of the tradeoff between steric and electronic factors. The latter promote 2,1-insertion due to differences in the distortion of the C−C and C−H bonds.[24] Thus, 2,1-insertion is observed in sterically undemanding systems, such as THF-back-olefin-front. On the contrary, increased steric congestion in the THF-back-olefin-back sites makes 1,2-insertion more feasible. Finally, the active sites with THF in the front position exhibit usually the highest insertion barriers.

The different reactivity of ethylene and propylene in the process of polymerization is caused by both steric and electronic factors. Higher barriers of propylene insertion compared to those of ethylene are related to steric interactions with THF, growing polymer chain, and the support. Considerable repulsion between the propylene methyl group and the support exists for the insertion transition state for propylene approaching the THF-back sites from the back position in the 2,1-mode of insertion. This interaction increases the external barrier noticeably and promotes 1,2-insertion over this kind of catalytic site, independently of the alkyl group attached to the titanium atom.

The activation barriers for the termination reaction, which involves β-hydrogen transfer (BHT) from the growing polymer chain to the monomer coordinatively bound to the titanium atom, were also calculated. The termination by β-hydrogen elimination was shown in a previous study[2] to have much higher barrier than the hydride transfer mechanism adapted here. The reaction limits the molecular weight of the resulting polyolefin. It probably does not quench the polymerization process itself, since its product (the π-complex) can still exhibit a certain catalytic activity.

The sites with the 2-butyl group simulating the polymer chain give rise to two paths of termination reaction, depending on the conformation of the chain. They lead to the formation of π-complexes of *cis*- and *trans*-2-butene, respectively. There is usually a significant difference between the heights of the corresponding two barriers. It is assumed that the particular conformations of the alkyl chain exist in equilibrium and interconvert easily; therefore, for each case only the lowest termination barrier is taken into account. It is also impossible to assign the termination transition states to the corresponding insertion transition states for the sites which have THF in the front position, since the olefin's carbon−carbon double bond is perpendicular to the metal−carbon bond. Therefore, the values of the respective barriers were placed arbitrarily in Table 1. Such an approach has no effect on the results of the following stochastic simulation.

It is obvious from Table 1 that the majority of termination barriers are at least 4−5 kcal/mol higher than the corresponding insertion barriers. This difference is even larger for the THF-front sites. In certain cases, however, especially for the sites with the 2-butyl chain, the termination occasionally becomes comparable with, or even preferred over, the insertion, which means that the occasional misinsertion (regioerror) may lead to a significant decrease in the molecular weight of the polymer produced.

The dormancy of active sites after propylene 2,1-insertion, postulated recently by Busico et al. for the heterogeneous[25,26] as well as single-site systems[27] and challenged by Landis et al.,[28] can be confirmed for the "edge" model in our classical ZN system. In this case, for the THF-back-olefin-back site, the lowest barrier for propylene insertion into a secondary polymeryl bond (represented here by 2-butyl group) amounts to 9.9 kcal/mol (Table 1), whereas the presence of a primary polymeryl bond (simulated by isobutyl group) reduces it by 3 kcal/mol. For *n*-propyl groups, which result from ethylene insertion, the respective barriers are even lower. On the contrary, there is no significant difference between propylene insertion into primary and secondary polymeryl bond in the case of the "slope" model. However, our stochastic approach indicates that only the "edge" model contributes to the overall catalytic activity (vide infra).

Thus, regioselectivity is controlled simultaneously by both factors mentioned above. Dormancy of secondary polymeryl bonds manifests itself in increased insertion barriers and acts against further insertion events preceded by a regioerror. Simultaneously, low termination barriers limit molecular weight of the resulting polymer and eradicate active sites bearing misinserted propylene mers.

Selection of the Most Productive Catalytic Sites

Up to this point, we have considered three possible kinds of transition states within two models. These transition states differ in the arrangement of the ligands (alkyl chain, THF, and olefin) in the titanium coordination sphere and originate from three separate titanium alkyl complexes (bare sites) with a free coordination site, listed in Table 2. Hence, the abundance of particular bare sites determines the concentration of the related π-complexes and transition states. This abundance can be estimated on the grounds of the relative energy of

Table 2. Bare Sites and Their Relative Energies for the "Slope" and "Edge" Models Treated Separately

bare site arrangement	free coordination site at	relative energy, kcal/mol
	"Slope Model"	
THF back, alkyl back	front	15.6
THF back, alkyl front	back	4.4
THF front, alkyl back	back	0.0
	"Edge Model"	
THF back, alkyl back	front	7.3
THF back, alkyl front	back	2.7
THF front, alkyl back	back	0.0

Table 3. Relative Average Rate of Propagation for Different Partial Pressures of Monomers

		activity		
model	active site	$p_e = 1.0$, $p_p = 0.0$	$p_e = 0.5$, $p_e = 0.5$	$p_e = 0.0$, $p_e = 1.0$
slope	*B*	1.9×10^{-4}	9.36×10^{-5}	1.57×10^{-6}
	F	4.20×10^{-8}	3.79×10^{-8}	3.99×10^{-10}
edge	*B*	1.00	8.19×10^{-1}	3.99×10^{-3}
	F	1.54×10^{-1}	1.21×10^{-1}	1.36×10^{-4}

the bare sites, given in Table 2, which allows us to exclude the THF-back-olefin-front sites from further considerations due to their low abundance and marginal role in the process of polymerization. The lower stability of these sites can be attributed to steric hindrance and mutual repulsive interaction between the Lewis base, alkyl chain, and the support.

The remaining two alkyl complexes, one with THF in the front position and one with THF in the back position (Figure 2), constitute two separate active sites. We shall refer to them as *F* and *B*, respectively. Our calculations indicate that the interconversion between them is difficult with a barrier larger than 15 kcal/mol.

It was very instructive to estimate the contribution of both models, i.e., "slope" and "edge" , to the polymerization process. First, we assessed the abundance of simple titanium alkyl complexes deposited on the support within both models by comparing the Gibbs free energies for the following reaction of formation:

$$(\text{support}) + TiCl_2CH_3 \rightarrow (\text{support})TiCl_2CH_3 \quad (4)$$

The values of ΔG for the "slope" and the "edge" alkyl complexes were equal to −4.5 and −8.3 kcal/mol, respectively. Using the Eyring equation, we can state that the concentration of the "edge" sites is 612 times higher than the "slope" ones. Taking into account this fact, as well as the activity data shown in Table 3, it is sensible to conclude that the polymer is produced mainly over the sites described by the "edge" model, even though the abundances of the (100) and (110) cuts of a $MgCl_2$ crystal cannot be equal. For these reasons, we shall analyze only the "edge" model by means of the stochastic approach.

Finally, we estimated the distribution of the *B* and *F* sites within the "edge" model by comparing their relative energies (see Table 2). Despite the fact that the *F* sites are 95 times more abundant, the activity of the *B* sites is significantly higher. Bearing in mind the fact that all the external insertion barriers have been calculated with respect to the most stable bare site (THF in front) and the differences between these barriers for the *B* and *F* sites are comparable with the differences in stability of respective bare sites, we suggest that the contributions of both sites to the polymerization process are almost equal.

Thus, we were able to select the most important catalytic sites from the multitude of suggested species and the following stochastic approach can be limited to the *B* and *F* sites within the "edge" model.

Stochastic Simulation and Copolymer Microstructure

The raw data presented in Table 1 need to be processed in order to provide useful information about the resulting polymer structure and molecular weight as a function of temperature, pressure, and the relative comonomer composition. According to the Cossee−Arlman mechanism,[29−31] the olefin moiety becomes incorporated into the polymer chain with one of the olefin carbon atoms bound to the transition metal atom. Hence, the first insertion of propylene into the $Ti-CH_3$ bond yields either the isobutyl or 2-butyl chain, depending on the mode of insertion (1,2- vs 2,1-), whereas the ethylene reaction leads to the *n*-propyl chain. From these considerations it is obvious that the single act of insertion is controlled by the earlier insertion event directly preceding it because the structure of the growing polymer chain immediately attached to the metal center has a significant influence on the insertion barriers, as can be seen from Table 1. Therefore, our model of polymerization obeys the principles of the Markov process.[32]

The algorithm of stochastic simulation applied in order to study polymer growth is based on the transition-state theory. It will now be illustrated for one of the sites within a particular model, where we have five possible insertion processes ($1 \le b \le 5$) for each end chain ($a = 1, 2, 3$). In the first step, the matrix of insertion reaction rates $r_{a,b}$ and termination rates $r_{T,a,b}$ for a selected site and the initial a value is calculated according to formula 3. Since it is assumed that the probability of a particular route of insertion is determined by the rate of this reaction relative to other possible routes of insertion and termination, the values of insertion rates are replaced by their relative ratios in the second step. The probability of a particular route of insertion is given by

$$p_b = \frac{r_b}{r_T + \sum_{b=1}^{5} r_b} \quad (5)$$

for $1 \le b \le 5$, where r_T is the cumulative termination rate for a particular site:

$$r_T = \sum_{b=1}^{5} r_{T,b} \quad (6)$$

The probability of termination is further given by

$$p_{T,b} = \frac{r_{T,b}}{r_T + \sum_{b=1}^{5} r_b} \quad (7)$$

Next, a uniform deviate (a random number between 0 and 1) is selected. In the example shown in Figure 6, if this number ranges between $p_1 + p_2 + p_3$ and $p_1 + p_2 +$

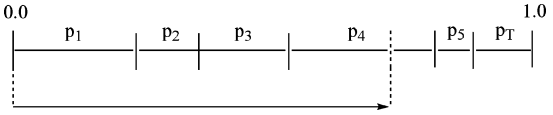

Figure 6. Relative probability of a chosen route of insertion.

Table 4. Percentage Composition of the Copolymer Obtained over the "Edge" Model for Different Partial Pressures of Comonomers

	$p_e = 0.5$, $p_p = 0.5$	$p_e = 0.2$, $p_p = 0.8$	$p_e = 0.1$, $p_p = 0.9$	$p_e = 0.05$, $p_p = 0.95$	$p_e = 0.0$, $p_p = 1.0$
		B Site			
ethylene	89.7	70.6	53.9	37.8	0.0
propylene 1,2-; *re*	0.4	1.0	1.6	2.1	4.2
propylene 1,2-; *si*	9.7	28.1	44.1	59.4	93.9
propylene 2,1-; *re*	0.1	0.2	0.4	0.7	1.8
propylene 2,1-; *si*	0.0	0.0	0.0	0.0	0.0
		F Site			
ethylene	84.6	67.1	57.6	50.3	0.0
propylene 1,2-; *re*	14.7	30.9	38.6	43.0	20.4
propylene 1,2-; *si*	0.1	0.2	0.3	0.5	16.0
propylene 2,1-; *re*	0.6	1.8	3.4	6.1	63.1
propylene 2,1-; *si*	0.0	0.0	0.0	0.1	0.5

$p_3 + p_4$, route 4 is selected. Conversely, if this number is greater than $p_1 + p_2 + p_3 + p_4 + p_5$, the simulation is terminated immediately.

For any catalytic site (*B* or *F*) within a given model, the insertion step will depend on the nature of the growing chain ($a = 1, 2, 3$). For a given choice of a, the insertion has five possible outcomes depending on the nature of the olefin (propylene or ethylene) as well as propylene orientation (*re* vs *si*) and insertion mode (1,2- vs 2,1-). The actual insertion process is chosen by calculating p_i ($1 \le i \le 5$) and performing a stochastic treatment (Figure 6). The process is repeated according to the new growing chain over and over again until a termination condition (vide supra) has been encountered.

The results of the stochastic simulations performed for a range of partial pressures of comonomers, presented in Table 4, indicate clearly that the insertion of ethylene is preferred for all the models studied. To support these data, we have calculated monomer reactivity ratios, defined as follows:

$$R_{C_2H_4} = \frac{k_{ee}}{k_{ep}} \tag{8}$$

$$R_{C_3H_6} = \frac{k_{pp}}{k_{pe}} \tag{9}$$

where k_{ee} and k_{pp} denote rate constants of homopolymerization of ethylene and propylene, whereas k_{ep} and k_{pe} are the rate constants of copolymerization (propylene following ethylene and ethylene following propylene, respectively). To simplify our calculations, we have assumed that propylene insertion has only one outcome; thus, the rates of insertion into the complexes with the 2-butyl and isobutyl groups have been summed up. The reactivity ratios of ethylene are all greater than 1, whereas those of propylene remain close to 0, as shown in Table 5. This means that ethylene is the monomer of higher reactivity, independently of the previous insertion event and the product of copolymerization tends to contain significant amount of C_2H_4 units. The reactivity ratios obtained in our simulation are in good agreement with numerous experimental works dealing with $MgCl_2$-supported Ti(III) catalysts,[33−36] based on either NMR analysis or classical copolymerization equations. The only difference is a slightly underestimated propylene reactivity ratio. As a result, the product of reactivity ratios is always less than 1.0, which indicates that the propylene mers in the polymer chain will occur as isolated units rather than blocks.

Table 5. Reactivity Ratios of Ethylene and Propylene over the "Edge" Model

active site	$R_{C_2H_4}$	$R_{C_3H_6}$	$R_{C_2H_4}R_{C_3H_6}$
B	8.49	0.07	0.5943
F	4.58	0.01	0.0458

Table 6. External Insertion Barriers for Propylene Insertion into the Ti−^{n}Pr Chain of the Δ and Λ Enantiomers of the *B* Site within the "Edge" Model

	$\Delta E^{\#}$ for enantiomer, kcal/mol	
insertion mode	Δ	Λ
1,2; *si*	4.7	7.0
1,2; *re*	6.8	4.6
2,1; *re*	8.0	12.0
2,1; *si*	12.9	7.5

The composition of the copolymer can be affected to some extent by varying reaction conditions. The chain becomes slightly enriched in the C_3H_6 units as the partial pressure of propylene in the reaction mixture is increased. Equimolar composition of both mers in the resulting copolymer can be attained for relatively high partial pressure of propylene, typically $p_p \approx 0.9$ (see Table 4).

The results shown in Table 4 suggest relatively good regioselectivity (≥96%) of the catalytic system under investigation. The 1,2-mode of insertion is predominant for all sites. However, this does not hold true for the *F* sites if pure propylene is polymerized. In such a case, 2,1-insertions constitute over 60% of all insertion events. It is important to note that the *n*-propyl chains attached to the titanium atom promote 1,2-insertion, whereas for branched chains, 2,1-insertion is preferred (see respective insertion barriers in Table 1). Ethylene, being more reactive, inserts easily into the Ti−C bond, forming linear alkyl chains. As long as a sufficient (though very small) amount of ethylene is present in the reaction mixture, the difference in the external barriers of ethylene and propylene is not compensated by high partial pressure of the latter. There is enough discrimination between ethylene and propylene that linear alkyl chains are formed in the vicinity of the titanium atom and 2,1-insertion is prevented. Conversely, when the concentration of branched chains in the polymer increases, the probability of misinsertions becomes more apparent. Even an occasional event of propylene 2,1-insertion changes the reactivity of the site and increases its propensity toward this mode of reaction, which leads to the series of subsequent 2,1-insertions. Thus, in polymerization of pure propylene, *F* sites promote this mode of reaction.

Our stochastic simulation indicate also a reasonable degree of stereoselectivity. A detailed analysis of data included in Table 4 reveals that the polymer obtained over the *B* site contains mainly the *si*-oriented mers, whereas the opposite is true for the *F* site. This is the result of an arbitrary choice of the particular enantiomer (Δ or Λ) of the catalytic species. Switching between the enantiomers reverses the trends in stereoselectivity (see Table 6).

The stochastic approach enabled us to calculate the values of molecular weight and construct the molecular

Table 7. Molecular Weight of the Copolymer Obtained over the "Edge" Model for Different Partial Pressures of Monomers

	$p_e = 0.5$, $p_p = 0.5$	$p_e = 0.2$, $p_p = 0.8$	$p_e = 0.1$, $p_p = 0.9$	$p_e = 0.05$, $p_p = 0.95$	$p_e = 0.0$, $p_p = 1.0$
B site	1.47×10^6	6.42×10^5	4.31×10^5	3.01×10^5	5.84×10^4
F site	4.44×10^6	5.78×10^5	1.57×10^5	4.74×10^5	5.77×10^2

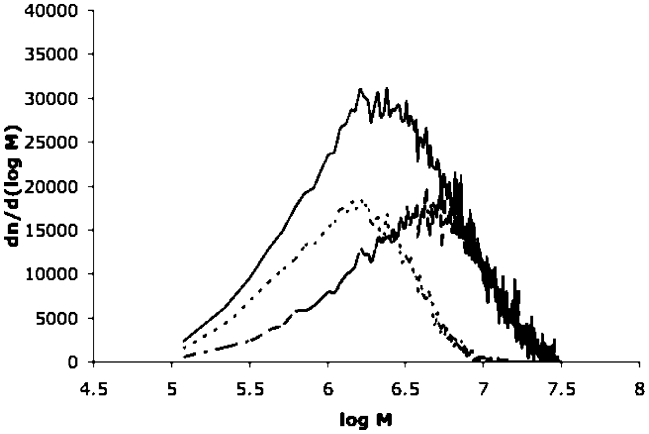

Figure 7. Molecular weight distribution for the copolymer produced over the "edge" model at equal partial pressures of monomers.

weight distribution curve for the copolymer. This time the stochastic simulation was run 20 000 times for each site. Since certain cases within the "edge" model exhibit extremely high termination barriers, often exceeding 20 kcal/mol, the competitive reactions leading to destruction of the active site (such as rearrangement, THF elimination, etc.) may play an important part in the process. Termination over the sites modified in this way, which are less crowded, may be more feasible. Therefore, it is reasonable to apply the cutoff of 14 kcal/mol for all termination barriers. The values of molecular weight obtained as a function of monomer concentration are given in Table 7. Both sites produce polymers of comparable molecular weight, and it is impossible to obtain pure propylene of high molecular weight. Instead, the oligomer is formed, especially over the *F* site. This fact can be rationalized by relatively high insertion barriers for the site with the 2-butyl group (whereas corresponding termination barriers remain constant after cutoff). Thus, any misinsertion giving rise to 2-butyl groups usually increases probability of termination in the stochastic model.

Our findings do not contradict what is usually observed experimentally for the classical ZN systems by many authors[25,26,37−39]—although the composition of copolymers (Table 4) calculated without analyzing molecular weight (Table 7) might suggest otherwise. It is believed that the polyolefins obtained over titanium-based catalysts consist only of 1,2-inserted mers, while 2,1-insertions lead either to easy termination and splitting of the polymer chain from the titanium atom or increased steric hindrance around the metal atom, which deteriorates catalytic activity. This happens in our simulation, where regioerrors raise insertion barrier and decrease the ratio of propagation to termination, thus lowering activity and molecular weight.

The molecular weight distribution for the copolymer obtained over the "edge" site using equimolar mixture of comonomers is shown in Figure 7. The two components drawn in dotted lines relate to the *B* sites ($M_n = 1.47 \times 10^6$; MWD = 1.97) and the *F* sites ($M_n = 4.44 \times 10^6$; MWD = 1.99). The final curve, drawn in solid line, represents the copolymer of $M_n = 2.95 \times 10^6$ and MWD = 2.49. The molecular weight distribution is now greater than 2.0, which corresponds to the multisite catalyst. However, since there are only two kinds of sites producing polymers of comparable molecular weight, the molecular weight distribution is not particularly wide.

Finally, it is worth mentioning that the regioselectivity and stereoselectivity for polypropylene obtained over the *B* site within the "edge" model, calculated according to the data presented in Table 4, are equal 98.2% and 95.7%, respectively.

Concluding Remarks

A comprehensive scheme of the copolymerization of ethylene and propylene over the "slope" and "edge" models of active site modified by THF as a Lewis base was built and applied. We were able to select the species responsible for the catalytic activity and to address the problem of microstructure of the resulting polymer. In particular, we have discussed regiospecificity and stereospecificity of the catalyst and molecular weight of the polymer. These properties are controlled by all the components of the catalytic system, i.e., the support, the Lewis base, and the growing polymer chain, which can modify Lewis acidity of the transition metal atom,[40] create steric hindrance around it, or influence chirality of the active site.

The active sites studied within this paper produce a copolymer, which is significantly enriched in ethylene units. The catalyst is not recommended for the homopolymerization of propylene due to its low activity toward this monomer, poor regioselectivity, and low molecular weight of the product. We have been able to demonstrate that moderate regio- and stereoselectivity can be attained with the system studied; nevertheless, the values calculated cannot compete with the experimental estimates for certain catalytic systems with multidentate ligands. Therefore, the natural extension of this work seems to aim in this direction and toward future rational design of new catalysts.

Our two models of active sites originate from two particular cuts of magnesium dichloride crystals. There is a number of possible cuts, exposing 3-, 4- 5-, and 6-coordinated magnesium atoms. The latter are of no importance to the catalytic process due to inability of binding the titanium species. It has been shown that the 3-coordinated magnesium atoms undergo rearrangement to form 5-coordinated species.[6] We have also demonstrated that the "slope" model based on such 5-coordinated magnesium is inactive and emphasized the importance of the "edge" model with 4-coordinated magnesium. This statement corresponds to the results obtained by Parrinello et al.,[6] although they concentrated mainly on the stability of active sites characterized by dynamical simulations.

The stochastic approach incorrectly predicts narrow molecular weight distribution. This is due to the fact that we restricted our considerations to only two sites, instead of four or five, as suggested in ref 41. However, one can imagine that THF is able to bind both to the titanium and magnesium atoms. Alternative structure with 4-coordinated magnesium can also be devised. Likewise, binuclear titanium species may exist, although the Gibbs free energy of their binding to the support is prohibitive according to our calculations. All

these considerations increase the number of possible models of active sites. Unfortunately, it would be impractical and expensive to study all of them. Bearing in mind the multisite character of heterogeneous catalysts, one should be aware of the complexity of the real system. Therefore, the model discussed within this paper reflects only a part of reality and demonstrates certain subset of properties.

Acknowledgment. The authors thank Randal Ford and Jeff Vanderbilt for helpful discussions and Eastman Chemical Co. for financial support. Z.F. thanks Yury V. Kissin and João B. P. Soares for their comments on polymer properties. T.Z. thanks the Canadian Government for a Canada Research Chair.

Supporting Information Available: Results of DFT calculations and stochastic simulations for the "slope" model as well as Cartesian coordinates of selected optimized structures. This material is available free of charge via the Internet at http://pubs.acs.org.

References and Notes

(1) Seth, M.; Ziegler, T. *Macromolecules* **2004**, *37*, 9191.
(2) Seth, M.; Ziegler, T. *Macromolecules* **2003**, *36*, 6613.
(3) Seth, M.; Margl, P. M.; Ziegler, T. *Macromolecules* **2002**, *35*, 7815.
(4) Markovits, A.; Minot, C. *Int. J. Quantum Chem.* **2002**, *89*, 389.
(5) Costuas, K.; Parrinello, M. *J. Phys. Chem. B* **2002**, *106*, 4477.
(6) Boero, M.; Parrinello, M.; Weiss, H.; Hüffer, S. *J. Phys. Chem. A* **2001**, *105*, 5096.
(7) Shiga, A. *J. Mol. Catal. A* **1999**, *146*, 325.
(8) Boero, M.; Parrinello, M.; Hüffer, S.; Weiss, H. *J. Am. Chem. Soc.* **2000**, *122*, 501.
(9) Monaco, G.; Toto, M.; Guerra, G.; Corradini, P.; Cavallo, L. *Macromolecules* **2000**, *33*, 8953.
(10) Cavallo, L.; Guerra, G.; Corradini, P. *J. Am. Chem. Soc.* **1998**, *120*, 2428.
(11) Boero, M.; Parrinello, M.; Terakura, K. *J. Am. Chem. Soc.* **1998**, *120*, 2746.
(12) Krentsel, B. A.; Kissin, Y. V.; Kleiner, V. J.; Stotskaya, L. L. *Polymers and Copolymers of Higher* α*-olefins*, Hanser/Gardener: Cincinnati, OH, 1997.
(13) Xu, J. T.; Feng, L. X.; Yang, S. L.; Wu, Y. N.; Yang, Y. Q.; Kong, X. M. *Macromol. Rapid Commun.* **1996**, *17*, 645.
(14) Becke, A. D. *Phys. Rev. A* **1988**, *38*, 3098.
(15) Perdew, J. P. *Phys. Rev. B* **1986**, *33*, 8822.
(16) Vosko, S. H.; Wilk, L.; Nusair, M. *Can. J. Phys.* **1980**, *58*, 1200.
(17) Krijn, J.; Baerends, E. J. Fit Functions in the HFS Method, Tech. Rep., Department of Theoretical Chemistry, Free University, Amsterdam, The Netherlands, 1984.
(18) Te Velde, G.; Bickelhaupt, F. M.; Baerends, E. J.; Fonseca Guerra, C.; Van Gisbergen, S. J. A.; Snijders, J. G.; Ziegler, T. *J. Comput. Chem.* **2001**, *22*, 931.
(19) Baerends, E. J.; Ellis, D. E.; Ros, P. *Chem. Phys.* **1973**, *2*, 41.
(20) Versluis, L.; Ziegler, T. *J. Chem. Phys.* **1988**, *88*, 322.
(21) Te Velde, G.; Baerends, E. J. *Phys. Rev. B* **1991**, *44*, 7888.
(22) Fonseca Guerra, C.; Snijders, J. G.; Te Velde, G.; Baerends, E. J. *Theor. Chim. Acta* **1998**, *99*, 391.
(23) Press, W. H.; Teukolsky, S. A.; Vetterling, W. T.; Flannery, B. P. *Numerical Recipes in Fortran 77. The Art of Scientific Computing*, 2nd ed.; Press Syndicate of the University of Cambridge: Cambridge, 1992.
(24) Michalak, A.; Ziegler, T. *Organometallics* **1999**, *18*, 3998.
(25) Busico, V.; Cipullo, R.; Polzone, C.; Talarico, G. *Macromolecules* **2003**, *36*, 2616.
(26) Busico, V.; Chadwick, J. C.; Cipullo, R.; Ronca, S.; Talarico, G. *Macromolecules* **2004**, *37*, 7437.
(27) Busico, V.; Cipullo, R.; Romanelli, V.; Ronca, S.; Togrou, M. *J. Am. Chem. Soc.* **2005**, *127*, 1608.
(28) Landis, C. R.; Sillars, D. R.; Batterton, J. M. *J. Am. Chem. Soc.* **2004**, *126*, 8890.
(29) Cossee, P. *J. Catal.* **1964**, *3*, 80.
(30) Arlman, E. *J. Catal.* **1964**, *3*, 89.
(31) Arlman, E.; Cossee, P. *J. Catal.* **1964**, *3*, 99.
(32) Bailey, N. T. J. *The Elements of Stochastic Processes with Applications to the Natural Sciences*, 3rd ed.; Wiley: New York, 1967.
(33) Kakugo, M.; Naito, Y.; Mizunuma, K.; Miyatake, T. *Macromolecules* **1982**, *15*, 1150.
(34) Chang, H.-S.; Song, W.-D.; Chu, K.-J.; Ihm, S.-K. *Macromolecules* **1992**, *25*, 2086.
(35) de Santa Maria, L. C. *Polymer* **1995**, *14*, 2845.
(36) Yoon, J.-S. *Eur. Polym. J.* **1995**, *31*, 999.
(37) Busico, V.; Cipullo, R. *Prog. Polym. Sci.* **2001**, *26*, 443.
(38) Chadwick, J. C. *Macromol. Symp.* **2001**, *173*, 21.
(39) Kissin, Y. V.; Rishina, L. A. *J. Polym. Sci., Part A: Polym. Chem.* **2002**, *40*, 1353.
(40) Flisak, Z.; Szczegot, K. *J. Mol. Catal. A* **2003**, *206*, 429.
(41) Kissin, Y. V. *J. Polym. Sci., Part A: Polym. Chem.* **2003**, *41*, 1745.

MA0516844